A low power high linearity baseband for a direct conversation CMMB tuner

Ma Heping(马何平)[1, †], Yuan Fang(袁芳)[1], Shi Yin(石寅)[1], Lan Xiaoming(兰晓明)[1], and Dai Fa Foster(代伐)[2]

(1 Institute of Semiconductors, Chinese Academy of Sciences, Beijing 100083, China)

(2 Department of Electrical & Computer Engineering, Auburn University, Auburn, AL 36849-5201, USA)

Abstract: An analog baseband circuit made in a 0.35-μm SiGe BiCMOS process is presented for China Multimedia Mobile Broadcasting (CMMB) direct conversion receivers. A high linearity 8th-order Chebyshev low pass filter (LPF) with accurate calibration system is used. Measurement results show that the filter provides 0.5-dB passband ripple, 4% bandwidth accuracy, and –35-dB attenuation at 6 MHz with a cutoff frequency of 4 MHz. The current steering type variable gain amplifier (VGA) achieves more than 40-dB gain range with excellent temperature compensation. This tuner baseband achieves an OIP3 of 25.5 dBm, dissipates 16.4 mA under a 2.8-V supply and occupies 1.1 mm^2 of die size.

Key words: CMMB; BiCMOS; low pass filter; temperature compensation; frequency calibration
DOI: 10.1088/1674-4926/30/6/065007 **EEACC:** 2220

1. Introduction

China Multimedia Mobile Broadcasting (CMMB) is a mobile television and multimedia standard developed and specified in Mainland China by the State Administration of Radio, Film, and Television (SARFT). It is based on the satellite and terrestrial interactive multiservice infrastructure (STiMi). The CMMB service operates in the S-band frequency with 25-MHz bandwidth in order to offer 25 video and 30 radio channels.

In order to handle both satellite and terrestrial reception, the CMMB tuner requires a very high input sensitivity and a wide dynamic range, which requires very low noise and high linearity; small form factor and low cost, which requires a high degree of integration; and a low power consumption. The baseband of a CMMB tuner has to meet a strict specification from system requirements: (a) an accurate calibration system is needed to maintain the precision cutoff frequency against process variations, temperature drift, and aging; (b) a sharp transition band and a large stopband attention, which are important for efficient adjacent channel rejection; (c) a reasonable Q (quality factor) value for good linearity, lower noise and low power consumption; (d) a small passband ripple to improve the frequency dependent I/Q mismatch; (e) a temperature independent characteristic over a wide dynamic range, which is critical to achieving simple and accurate RSSI estimations. In Ref. [3], an active-RC filter and an automatic tuning system have been implemented, but these consume more power and a greater silicon area due to their complexity. In Ref. [5], the bandwidth of operational amplifier was estimated in order to decrease the power dissipation. In our work, the Q increase, which resulted from a poor bandwidth operational amplifier, is discussed. The results are important in low-power filter design. The variable gain amplifier with gain and temperature compensation and the low pass filter with accurate calibration system are described.

2. Baseband design

In a direct conversation architecture, optimal signal conditioning requires that gain and filter stages be alternated in the signal path, as shown in Fig. 1. The first stage after the mixer is an eighth-order Chebyshev low pass filter (LPF), so, it can thoroughly reject the adjacent channel interference and the high-frequency mixer intermodulation. This LPF can relax the linearity specifications of the following block and naturally decrease the power consumption. It also meets the ADC aliasing constrain. The LNA and the mixer of the tuner have a sufficient gain; so, the main filter has a sufficiently low noise to be used immediately behind the mixer. However, the filter itself should be very linear. The DCOC loop is used to remove DC offsets introduced by the mixer and the layout, which is discussed in detail in another paper related to this work.

2.1. Baseband variable gain amplifier

A VGA with temperature independent characteristic is

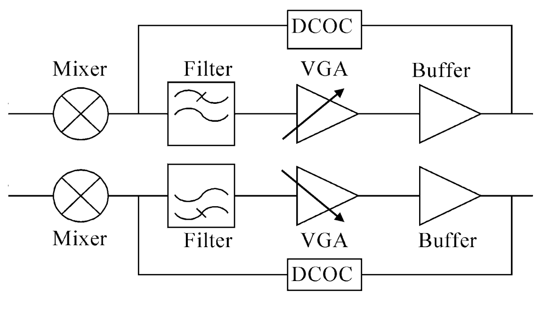

Fig. 1. Baseband chain.

† Corresponding author. Email: hpma@semi.ac.cn
Received 3 December 2008, revised manuscript received 9 January 2009

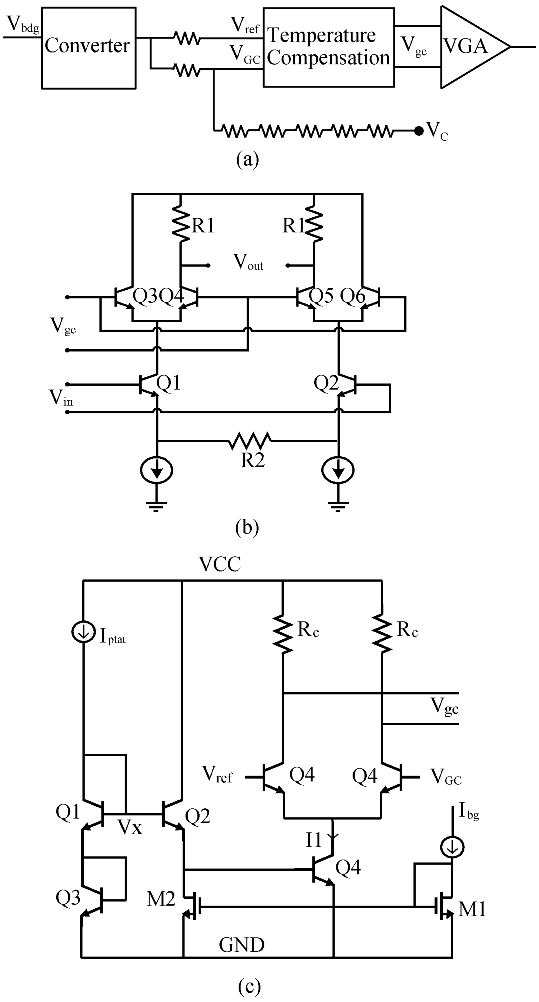

Fig. 2. (a) Detailed circuit schematic of AGC; (b) Detailed circuit schematic of VGA; (c) Detailed circuit of temperature compensation.

preferred in the CMMB tuner because of its large dynamic control range. We describe a SiGe BiCMOS VGA with accurate temperature compensation. A block diagram of the proposed VGA system is shown in Fig. 2(a). $V_{\rm bdg}$ is a constant voltage reference generated by a bandgap, and it is converted to a voltage reference $V_{\rm ref}$ by a voltage converter. $V_{\rm C}$ is the external control voltage from the digital baseband, and it changes to the internal control voltage $V_{\rm GC}$. Through these resistors, the voltage control range can be enlarged. The detailed circuit schematic of the VGA is illustrated in Fig. 2(b). The relation of gain and control voltage $V_{\rm gc}$ can be expressed as[1]

$$\frac{V_{\rm out}}{V_{\rm in}} = \frac{1}{1+{\rm e}^{-V_{\rm gc}/V_{\rm T}}}\frac{R_1}{R_2+1/g_{\rm m}}. \tag{1}$$

Equation (1) shows that the logarithmic gain (in dB) is almost linearly dependent on the control voltage $V_{\rm gc}$, when $V_{\rm gc}$ is both negative and has an absolute value less than the threshold voltage $V_{\rm T}$[1]. In addition, the gain is also related to the temperature mainly through $V_{\rm T}$, which causes the gain coefficient to vary with the temperature and is undesirable.

The temperature compensation can be done as shown in Fig. 2(c)[2]. Then, with the compensated voltage $V_{\rm gc}$ generated by the AGC circuit, the temperature variations can be compensated. The pivotal component of this stage is a current component that varies with the square of the absolute temperature. The intrinsic voltage loop is composed of transistors Q1, Q2, Q3, and Q4. The current flowing through Q1 and Q3 is proportional to the absolute temperature ($I_{\rm ptat}$), while that flowing through Q2 is derived from a constant current ($I_{\rm bg}$). Summing the voltages across the loop gives:

$$V_{\rm x} = V_{\rm T}\ln\frac{I_{\rm ptat}}{I_{\rm S1}} + V_{\rm T}\ln\frac{I_{\rm ptat}}{I_{\rm S3}} = V_{\rm T}\ln\frac{I_{\rm C2}}{I_{\rm S2}} + V_{\rm T}\ln\frac{I_{\rm C4}}{I_{\rm S4}}. \tag{2}$$

Thus I_1 shown in Fig. 2(c) is derived as

$$I_1 = I_{\rm C4} = \frac{I_{\rm ptat}^2}{I_{\rm C2}}\frac{I_{\rm S2}I_{\rm S4}}{I_{\rm S1}I_{\rm S3}} = \frac{I_{\rm ptat}^2}{I_{\rm bg}}\frac{I_{\rm S2}I_{\rm S4}}{I_{\rm S1}I_{\rm S3}}. \tag{3}$$

The factor $\frac{I_{\rm S2}I_{\rm S4}}{I_{\rm S1}I_{\rm S3}}$ depends only on the matching between transistors. So, the current I_1 is proportional to the square of the absolute temperature. Assuming that the transistors Q5 and Q6 are identical, we can get the output voltage of the differential pair as:

$$V_{\rm gc} = \alpha_{\rm F}I_1\tanh\left(\frac{V_{\rm ref}-V_{\rm GC}}{2V_{\rm T}}\right) \approx \alpha_{\rm F}I_1\frac{V_{\rm ref}-V_{\rm GC}}{2V_{\rm T}}, \tag{4}$$

where $\alpha_{\rm F} = \frac{\beta_{\rm F}}{1+\beta_{\rm F}}$, $\beta_{\rm F}$ is the forward current gain, and $V_{\rm ref}$ is a reference voltage that is independent of the temperature.

The latter equation holds when $\frac{V_{\rm ref}-V_{\rm GC}}{2V_{\rm T}} \ll 1$. Combining Eqs. (4) and (1) and according to $I_1 \propto T^2$, which can attenuate the "$V_{\rm T}$", the temperature compensation is provided by the current proportional to the square of the absolute temperature.

2.2. Baseband filter

In the baseband of the CMMB tuner, there are several major issues when we design an LPF. Regarding the selection of the LCR prototype, there are concerns of filter rejection response and group delay distortion. Owing to the very stringent adjacent-channel rejection specification and the ability to tolerate a nonuniform group-delay response, Chebyshev filters are more suitable although they have a high quality factor and consume a lot of power. In this paper, we have to estimate the accurate bandwidth of an operational amplifier in order to mitigate redundant power dissipation. Among $G_{\rm m}$-C, MOSFET-C, and active-RC filters, the linearity of $G_{\rm m}$-C filters is the worst. For low-power applications, MOS-resistors of the MOSFET-C operate in the so-called triode region and act as nonlinear resistors with deteriorated linearity. One method to improve the linearity is by using on-chip charge pumps to increase the gate voltage of the MOSFETs. However, this can only partially solve the problem. In addition, compared with a cascade of biquard to compose a high order filter, the leapfrog technique has a lower sensitivity against component value variations. In order to decrease the passband sensitivity, which results from the element, the leapfrog technique is used to synthesize the filter, and the configuration of the filter is obtained from the RLC ladder prototype. The structure of the BB filter is shown in Fig. 3(a)[3]. A 5-bit programmable binary-

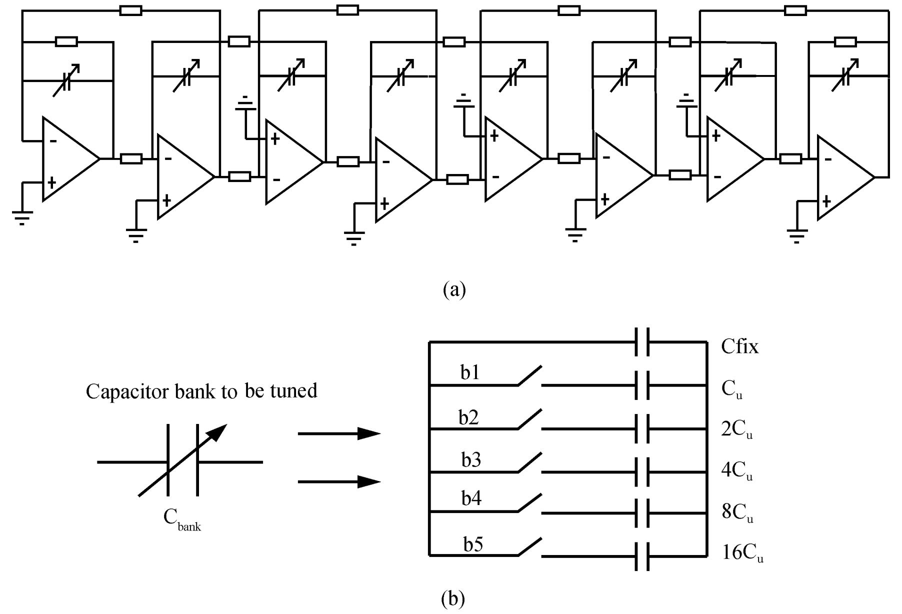

Fig. 3. (a) Structure of the BB filter; (b) A programmable capacitor bank.

weighted capacitor array [Fig. 3(b)] with a ±50% programmable range was employed to calibrate the process and the temperature drift.

As shown in Fig. 3(b), the capacitance of the capacitor bank is determined by a digital control word and can be tuned to a set of discrete values:

$$C_{\text{bank}} = C_{\text{fix}} + nC_{\text{u}}, \quad n = 0, \cdots, 2^N - 1, \tag{5}$$

where C_{fix} and C_{u} are a fixed capacitor and a unit capacitor, respectively. Each capacitance bank must be capable of representing every capacitance value in a specified range given by $C_{\text{nom}} \pm x\%$. C_{nom} is the nominal design value, and x is the required percentage range of the capacitance. We have Eq. (6):

$$C_{\text{fix}} = C_{\text{nom}}\left[1 + \frac{x}{100}\left(\frac{1}{2^N} - 1\right)\right]. \tag{6}$$

We choose a tuning range of (–50%, +50%) around C_{nom}. The quantization error ε is given by

$$\varepsilon = \pm\frac{1}{\dfrac{2C_{\text{fix}}}{C_{\text{u}}} + 2n \mp 1}. \tag{7}$$

The quantization error ε will be maximized when n equals zero. The calculation shows that the maximum $\varepsilon_{\max}$ is ±3.125% ($\varepsilon_{\max} = 1/2^N$, $N = 5$). The tuning accuracy is within ±3.125%, i.e., it has a ±125 kHz variation for the 4 MHz cutoff frequency.

Here, we will analyze the Q increase problem, which depends on the bandwidth of the amplifier. In order to estimate the necessary GBW for the OPAMP, a second-order filter is analyzed, as shown in Fig. 4.

The transfer function of a nonideal amplifier is expressed as

$$A(s) = \frac{A_{\text{amp}}w_{\text{amp}}}{s + w_{\text{amp}}}. \tag{8}$$

If we suppose that this nonideal amplifier is used in the lossy

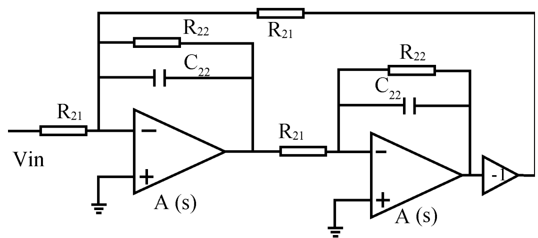

Fig. 4. Second-order low pass filter.

integrator shown in Fig. 4, the transfer function $H(s)_{\text{lossy}}$ is derived as

$$H(s)_{\text{Lossy}} \approx \frac{1}{R_{21}}\frac{1}{\dfrac{1}{R_{22}} + sC_{22} - \dfrac{w^2C_{22}}{A_{\text{amp}}w_{\text{amp}}}}. \tag{9}$$

We can derive the Q increase of the filter due to the amplifier's nonideality. We define ΔQ_2 as

$$\Delta Q_2 = \frac{Q_{\text{L}} - Q_{\text{I}}}{Q_{\text{I}}}, \tag{10}$$

$$\frac{Q_{\text{L}} - Q_{\text{I}}}{Q_{\text{I}}} \approx \frac{1}{A_{\text{amp}}w_{\text{amp}}/2w_{\text{I}}Q_{\text{I}} - 1}. \tag{11}$$

Q_{L} is the Q factor of the lossy integrator, which has a nonideal amplifier; Q_{I} is the Q factor of the integrator with an ideal amplifier. W_{I} is the bandwidth of the filter. The Q is defined as the gain at the cutoff frequency.

As the GBW decreases, the Q of the filter increases abruptly from the Q of its LCR prototype. The required GBW for the Chebyshev filter is twice as high as the GBW for the Butterworth filter. Higher Q filters, such as Chebyshev filters, require a higher GBW to mitigate the increase of Q from their LCR prototype. In a 4 MHz 8th Chebyshev, in order to keep the increase of the Q (ΔQ_2) smaller than 5 % (= 0.42 dB), the GWB must be 280 ($Q_{\max} = 7$) times as large as the cutoff frequency at 4 MHz. So, the GBW of the amplifier is not less than 1.12 GHz, and Equation (11) can be applied to high-order filters.

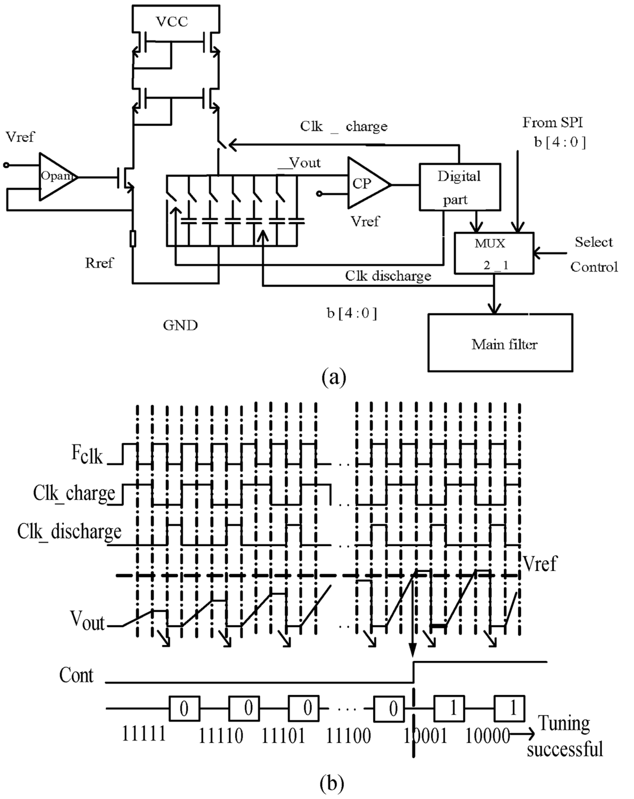

Fig. 5. (a) Calibration circuit schematic for the BB filter; (b) Operation of calibration.

The implementation of the OPAMP is a typical two-stage miller-compensation an OPAMP with common feedback circuit. The simulation shows that the OPAMP can achieve a GBW of 1.1 GHz, a phase margin of 70°, a DC gain of 75 dB, and a power consumption of 1.4 mW with a load capacitor of 500 fF (i.e., the parasitic capacitor value of the capacitor-bank in the main filter, which is less than 10% of the total value of the capacitor-bank) and a load resistor of 10 kΩ.

2.3. Automatic frequency tuning for filters

In a continuous-time active-RC filter, to guarantee the high-precision filtering operation, the accurate absolute values of the resistors and capacitors must be realized and maintained during operation. Figure 5(a) shows the block diagram of the general 5-bit tuning circuit for active-RC filters. The tuning system is based on a discrete capacitor bank and can be tuned either automatically or by switching the signal select within the device mux (multiplexer) high or low, as shown in the figure. The tuning system is mainly composed of the integrator, the comparator, and the digital part. The reference resistor and the capacitor bank should be chosen to be of the same kind as the main filter. The refer voltage is supplied by a bandgap-voltage reference, and the $V_{\rm ref}$ can be converted into a current by the constant-$G_{\rm m}$ architect. The current is accurately mirrored to charge the capacitor bank and this realizes the function of an integrator. The output voltage of an integrator can be expressed as

$$V_{\rm o} = \frac{V_{\rm ref}}{R_{\rm ref}C_{\rm bank}}t. \tag{12}$$

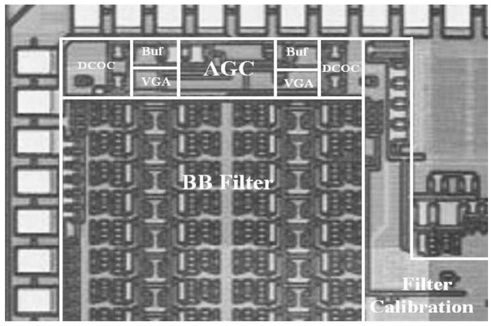

Fig. 6. Die photograph of the baseband RFIC.

The integrator output is compared with the reference voltage. If $V_{\rm ref} > V_{\rm o}$, the comparator outputs a high voltage, and the digital part decreases the 5-bit tuning code of the capacitor bank until $V_{\rm ref} < V_{\rm o}$. If $V_{\rm ref} < V_{\rm o}$, the comparator output voltage (Cont) is low, and the digital part stops to decrease the tuning code. This process moves $V_{\rm o}$ close to $V_{\rm ref}$. After every comparison, the signal Clk_discharge will discharge the integrator voltage on the capacitor bank, while Clk_charge gives the beginning signal to charge the capacitor bank when a new tuning code has been generated[4, 5].

The operation of the tuning is shown in Fig. 5(b). The tuning process occurs in the serial manner. In the initial state, all the tuning control bits are high and all feedback capacitors are connected, implying the minimum slope of the integrator output. The control bits and corresponding capacitors sequentially become low and disconnect from the circuit, respectively. At the moment when the slope is large enough for the output to reach the reference value during the Clk_charge, the tuning process is finished. In this way, the worst-case total number of clock cycles for tuning operation is 2^N for a tuning accuracy of N bit. The tuning system can be turned off after tuning.

3. Measurement result

Figure 6 gives the die photograph of the CMMB baseband. The baseband of the CMMB is implemented in a 0.35 μm SiGe BiCMOS technology, which occupies 1.1 mm^2 of die size.

Figure 7(a) shows the measured and the simulated VGA gain versus the control voltage at 2.8 V and 25 degrees. The measured curve is similar to the simulated curve. Figure 7(b) gives the measured and simulated VGA gain curves at 2.52 V and 85 degrees. Though the curves are slightly shifted, the gain range can meet the system requirement.

The measured frequency AC characteristics of the filter are illustrated in Figs. 8(a) and 8(b). The filter shows a cut-off frequency of 4.28 MHz at 25 degrees and 4.13 MHz at 85 degrees with a corner frequency calibration.

Figure 9 shows the measured in-band OIP3. The experimental result is measured with the VGA gain of 8 dB. The input power is –22 dBm. Therefore, the in-band OIP3 is 5.7 dBm according to Eq. (13). In addition, the measured out-of-band OIP3 is 25.5 dBm.

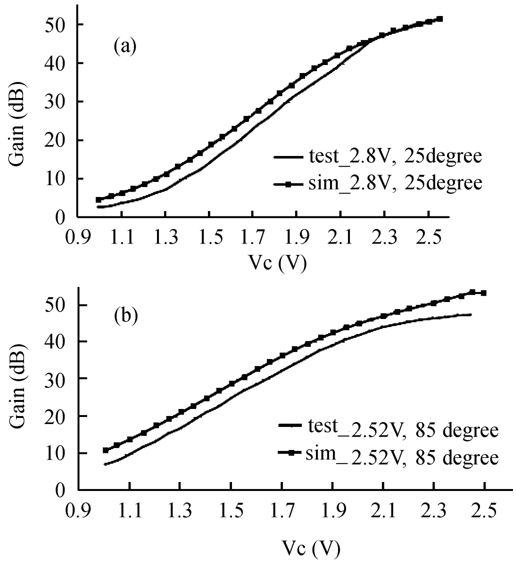

Fig. 7. Measurement and simulation results of the VGA gain: (a) At 25 degrees and 2.8 V; (b) At 85 degrees and 2.52 V.

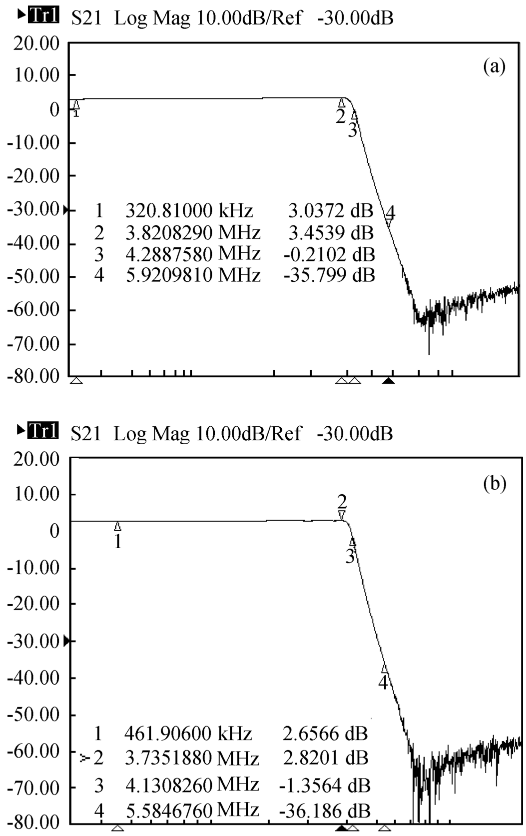

Fig. 8. Measured frequency characteristics of the filter with the calibration result: (a) At 25 degrees; (b) At 85 degrees.

$$\mathrm{IIP}_3|_{\mathrm{dBm}} = \frac{\Delta P|_{\mathrm{dBm}}}{2} + P_{\mathrm{in}}|_{\mathrm{dBm}}. \tag{13}$$

Table 1 summarizes the CMMB baseband performance.

4. Conclusion

This paper presents a low power baseband for China Multimedia Mobile Broadcasting applications. It was realized in 0.35-μm SiGe BiCMOS technology. Excellent temperature compensation and an accurate calibration system have been successfully realized. The main filters achieve a good linearity and have low power dissipation. The measurement results show that the baseband satisfies the CMMB tuner specifications.

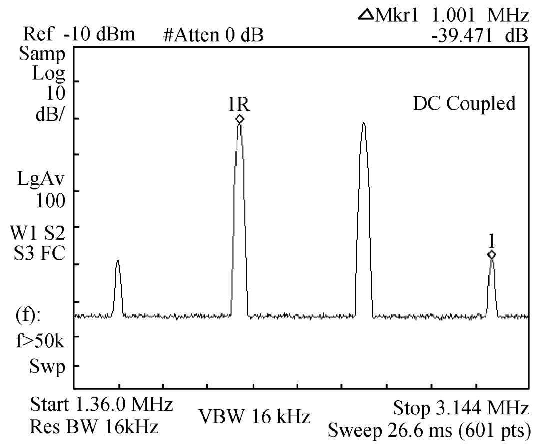

Fig. 9. Measured in-band OIP3 of 5.7 dBm.

Table 1. Summary of the CMMB baseband performance.

Parameter	Measured value
Gain range	> 40 dB
3 dB bandwidth	4.28 MHz
Attenuation	35 dB @ 6 MHz
Passband ripple	0.5 dB
In-band OIP3	5.7 dBm
Out-of-band OIP3	25.5 dBm
Supply voltage	2.8 V
Current consumption	16.4 mA
Area	1.1 mm^2

Acknowledgment

The authors wish to thank Yan Jun and Wen Dongmei for their encouragement and support.

References

[1] Riihihuhta H, Halonen K, Koli K. A high dynamic range 100 MHz AGC-amplifier with a linear and temperature compensated gain control. Circuits and Systems, 1994, 5: 521

[2] Hwang M W, Beck S, Min S, et al. A 1.8 dB NF 112 mW single-chip diversity tuner for 2.6 GHz S-DMB applications. IEEE International Solid-State Circuits Conference, 2006: 33.6

[3] Kousai S, Hamada M. A 19.7 MHz, fifth-order active-RC Chebyshev LPF for draft IEEE802.11n with automatic quality-factor tuning scheme. IEEE J Solid-State Circuits, 2007, 42(11): 2326

[4] Cho Y, Lim J, Jung K. Fast on-chip tuning circuit for active-RC filters using the SAR scheme. Circuits and Systems, 2005, 2: 1522; Razavi B. RF microelectronics. Pearson Education, Inc, 2003

[5] Du D, Li Y, Wang Z. An active-RC complex filter with mixed signal tuning system for low-if receiver. Circuits and Systems, 2006: 1031